Mapping Active Faults in Southern California in 3D Using Small Earthquakes: Southern San Andreas, San Jacinto, and Elsinore Fault Systems.

Award # 03HQGR0071

John Suppe
Department of Geosciences
Princeton University
Princeton, NJ 08544
609-258-4199(phone), 609-258-1274(fax)
suppe@princeton.edu

Program Elements I & III
Key Words: Neotectonics, Tectonic Structures, Seismotectonics, Regional Seismic Hazards.

Investigations

We have mapped active faults in southern California from the Mexican border north to the latitude of San Clemente (southern Orange County, N33.88°)(Fig.1a) based on the locations of small earthquakes and surface breaks of faults, concentrating on the San Jacinto and southern San Andreas fault systems. We evaluated several earthquake catalogs and procedures for optimal fault imaging, including double-difference relocation and clustering. Our best fault imaging is based on the more than 73,000 earthquakes from the catalog of relocated 1981-1998 earthquakes of Hauksson (2000), which has improved absolute locations based on an improved 3D velocity model in Southern California. A clustering algorithm was then applied to the relocated earthquake dataset in order to obtain tighter earthquake clouds and thus better-defined fault surfaces (Fig.1b). The earthquake datasets then were imported into Gocad 3D modeling software which allow us to separate earthquakes into coplanar clusters associated with different faults and fault strands and to fit optimized surfaces to them. We also imported the surface breaks of Alquist-Priolo fault zone dataset into Gocad in order to get better constraint for fault models at the surface. Finally, we compared imported focal mechanisms from the catalog of Hauksson (2000) into Gocad (with collapsed locations) in order to identify: [1] principal and auxiliary nodal planes, [2] fault surfaces that only have few earthquakes associated with them, [3] the slip direction of most faults.

Results

[1]. The imaging of faults has been dramatically improved by clustering (collapsing) earthquake locations. For example, the Figure 2 shows that the earthquake clouds including aftershocks of Superstition Hills and Elmore Ranch earthquakes get tighter and more coplanar in 3D, which for steeply dipping faults appears as concentrated lineations in the map view. This substantial improvement of fault imaging from relative earthquake locations combining with the precise surface-break data (Alquist-Priolo dataset) allows us to easily fit optimized surfaces to them.

[2]. Sixty active faults and fault segments have been mapped in this area (Fig.3a). The most

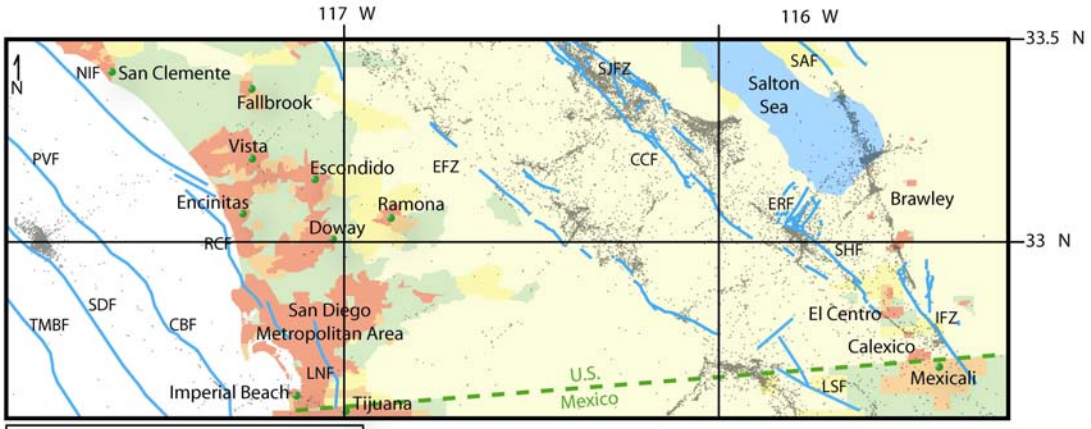

Figure 1a. Map of population density in the area of interest. The collapsed earthquake hypocenter locations of Hauksson [2000] and major fault zones are also shown for reference. SAF=San Andreas Fault, PVF=Palos Verdes Fault, RCF=Rose Canyon Fault, TMBF=Thirty Mile Bank Fault, SDF=San Diego Fault, SJFZ=San Jacinto Fault Zone, SHF=Superstition Hills Fault, ERF=Elmore Ranch Fault, IFZ=Imperial Fault Zone, CCF=Coyote Creek Fault, CBF=Coronado Bank Fault, LNF=La Nacion Fault, EFZ=Elsinore Fault Zone, LSF=Laguna Salada Fault, NIF=Newport Inglewood Fault.

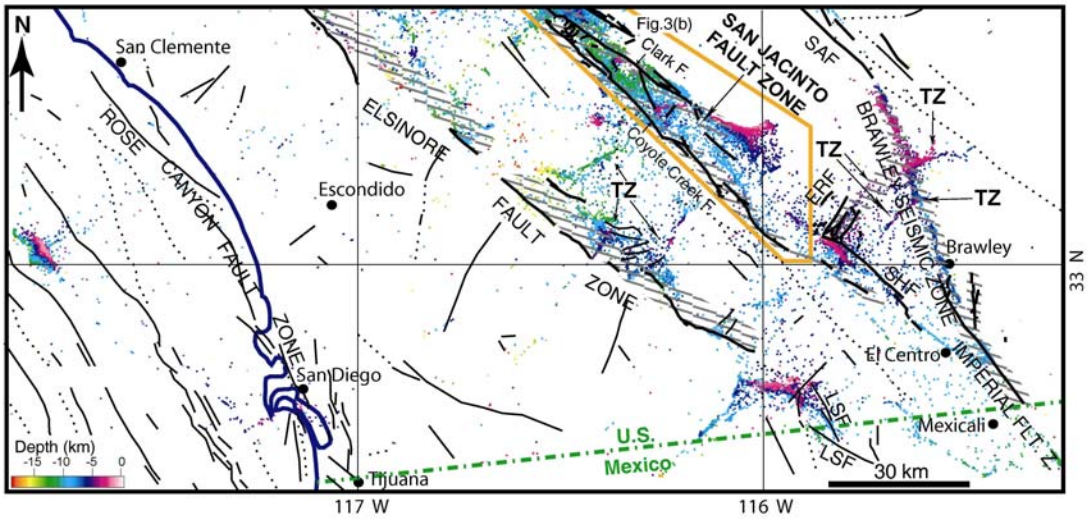

Figure 1b. Map of the collapsed hypocenter locations of the period 1981-1998 [Hauksson, 2000]. SAF=San Andreas Fault, LSF=Laguna Salada Fault, ERF=Elmore Ranch Fault, SHF=Superstition Hills Fault. TZ indicates the SW-NE trending fault zone.

striking feature is that in map view the seismicity, which is dominated by earthquakes near the base of the seismogenic zone at depths of ~10-15km, tends to form lineations which follows rather closely the surface fault traces after relocation, including Imperial, Superstition Hills, Elmore Ranch, Coyote Creek and Clark faults (Fig.1b, 2). The majority of this deep seismicity shows frequency-magnitude relationships characteristic of creeping faults and is well located in map view within the defined surface fault zones (modified from Jennings (1994), Fig.1b). This feature leads us to generate optimized fault models that are constrained largely by seismicity at the base of the seismogenic zone and by surface breaks. These observations suggest that many of these fault zones have a simple fault geometry that is largely locked. However some fault zones

show more complex behavior, particularly parts of the San Jacinto fault zone, which has scattered earthquake patterns within the defined fault zone and clearly shows several complexities in fault segments such as those between Coyote Creek and Clark faults (see Fig.1b [blue box] and Fig.3b, a close look of fault models within the San Jacinto fault zone [preliminary result]). The San Jacinto fault zone requires more work to illuminate these details in 3D.

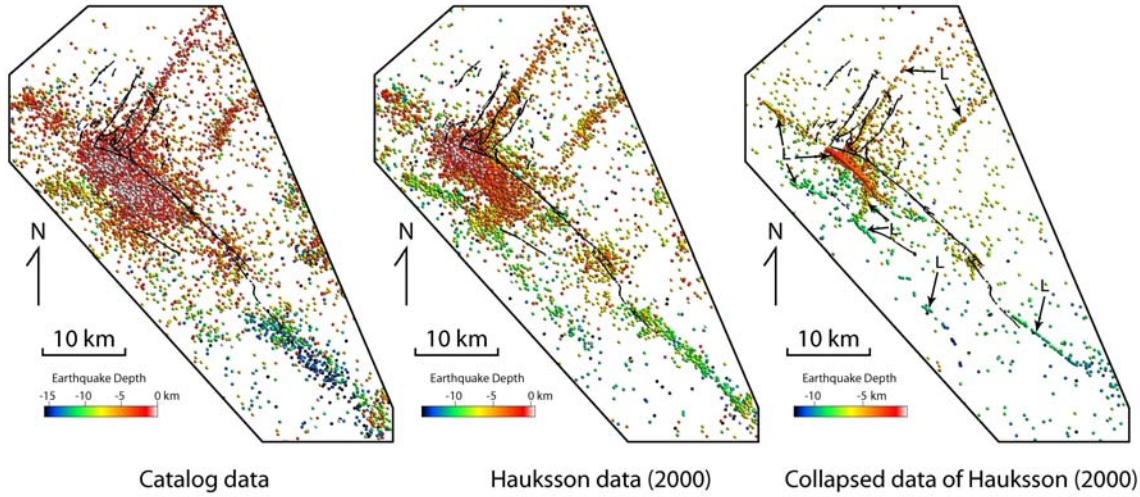

Figure 2. Map view of improved relative locations of earthquakes by using collapsing algorithm, an example of Superstition Hills and Elmore Ranch faults. L is the dense lineation of seismicity illuminated after collapsing.

[3]. Another interesting feature is the orthogonal fault patterns {the NW-SE trend for main fault zones and the NE-SW trend (TZ in the Fig.1b) for minor faults such as Elmore Ranch (Hudnut et al., 1989 and Nicholson et al., 1986) and others pointed out in Fig.1b}. After relocation, this orthogonal pattern is clearly illuminated and shown in not only the famous example of Superstition Hills and Elmore Ranch fault pair but several unnamed minor faults of the Brawley seismic zone and Elsinore fault zone as well. A detailed fault model of conjugate faults is shown in Fig.4 (Superstition Hills and Elmore Ranch fault pair).

[4]. The comparison between focal mechanisms and fault models is shown in Fig.5 (Imperial fault). Selected nodal planes of focal mechanisms with relocated locations show the sub-parallelism with the fault surface and the slip direction from the selected nodal planes indicates the right-lateral motion of Imperial fault, as expected (the earthquake data we used here just represent interseismic period for Imperial fault). It is worth noting that the earthquakes show the typical pattern of concentration at the base of the seismogenic zone, clustered within 9-10km in depth, as also shown by recent relocation by waveform cross correlation of Shearer.

[5]. Basically, there are two types of seismicity distribution within fault surfaces. One has earthquake clouds concentrated near the base of the seismogenic zone. For this type there are very few or no earthquakes between the earthquake clouds and surface fault traces, for example Imperial fault (Fig.5, also see point [4]), Elmore Ranch fault, Superstition Mountain fault and a deeper fault of northern San Jacinto fault zone near Anza. The other type of seismicity distribution has earthquakes rather smoothly distributed within the fault from the surface trace to

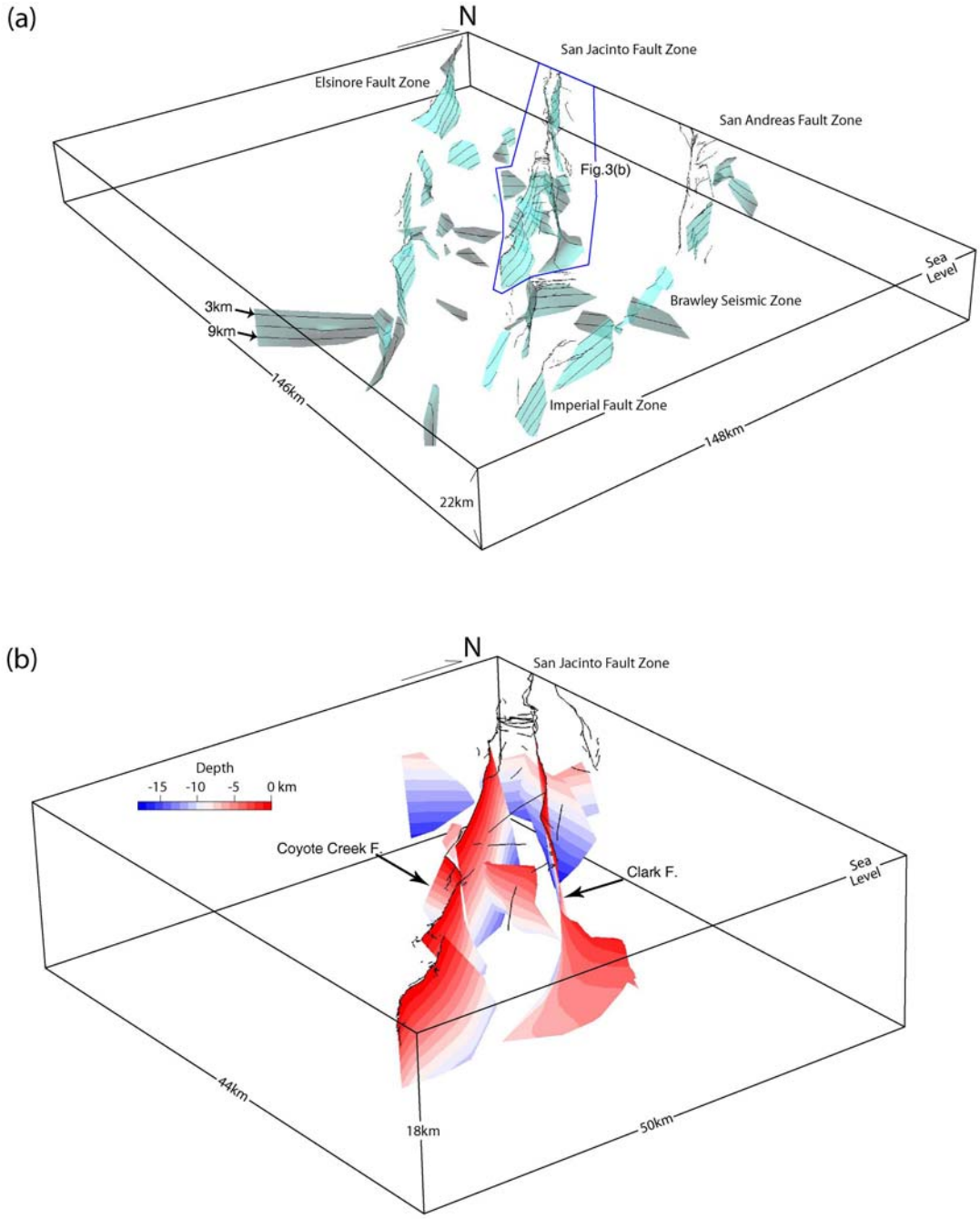

Figure 3. (a). Perspective view of the faults shown in Fig.1b. (b). Perspective view of zooming into the San Jacinto fault zone.

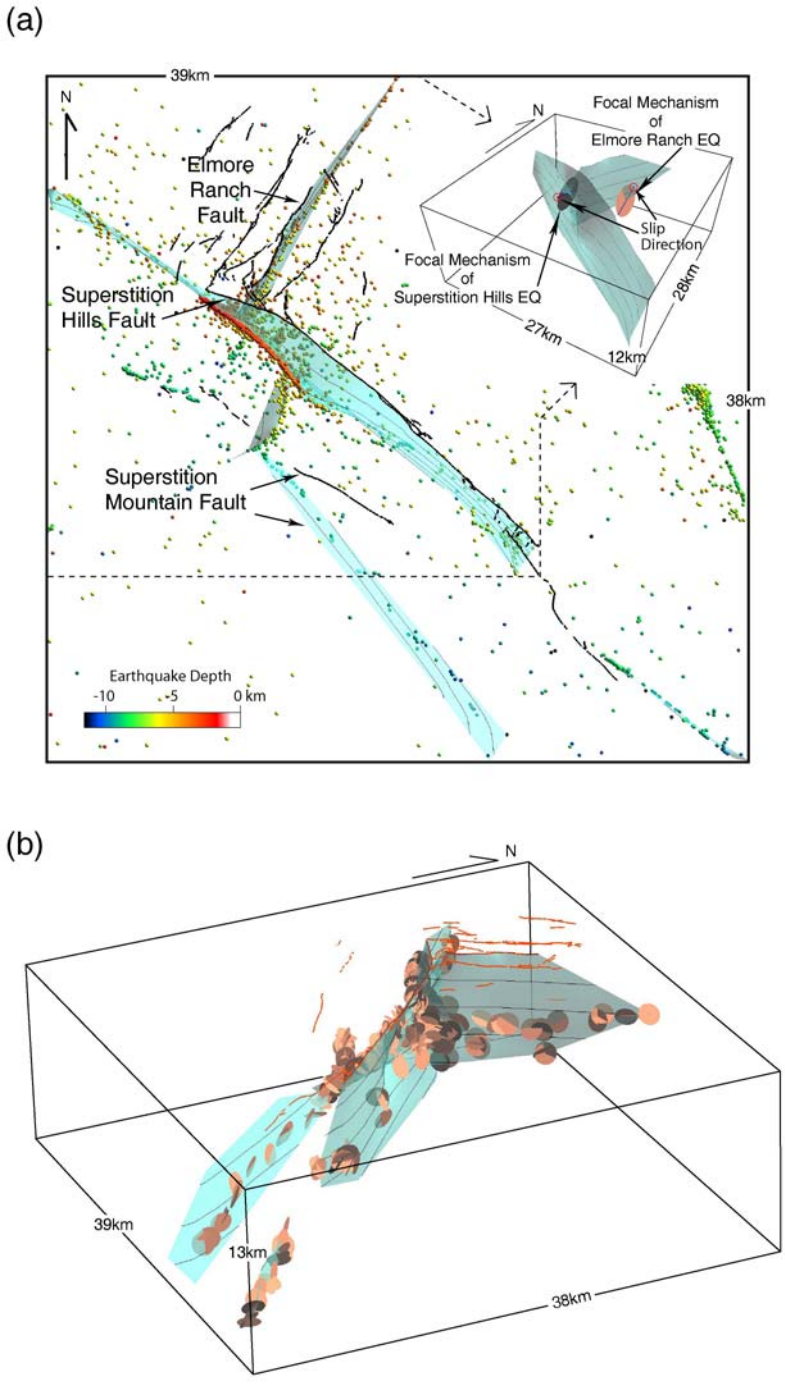

Figure 4. (a). Map view of the conjugate fault pattern, an example of Superstition Hills and Elmore Ranch fault pair. Fault models are rigorously constrained by collapsed earthquakes and the 1987 surface break. It is worth noting that the Elmore Ranch fault has a complicated parallel array of surface breaks, only one of which is illuminated by significant underlying seismicity (Fig.2). A perspective view in the upper-right corner shows how well two main focal mechanisms agree with fault surfaces. Two nodal planes have a diameter of 2400m. (b). Perspective view of fault surfaces and selected nodal planes showing the agreement between them. All planes have a default diameter of 800m. The interval of fault contours is 2 km in both (a) and (b).

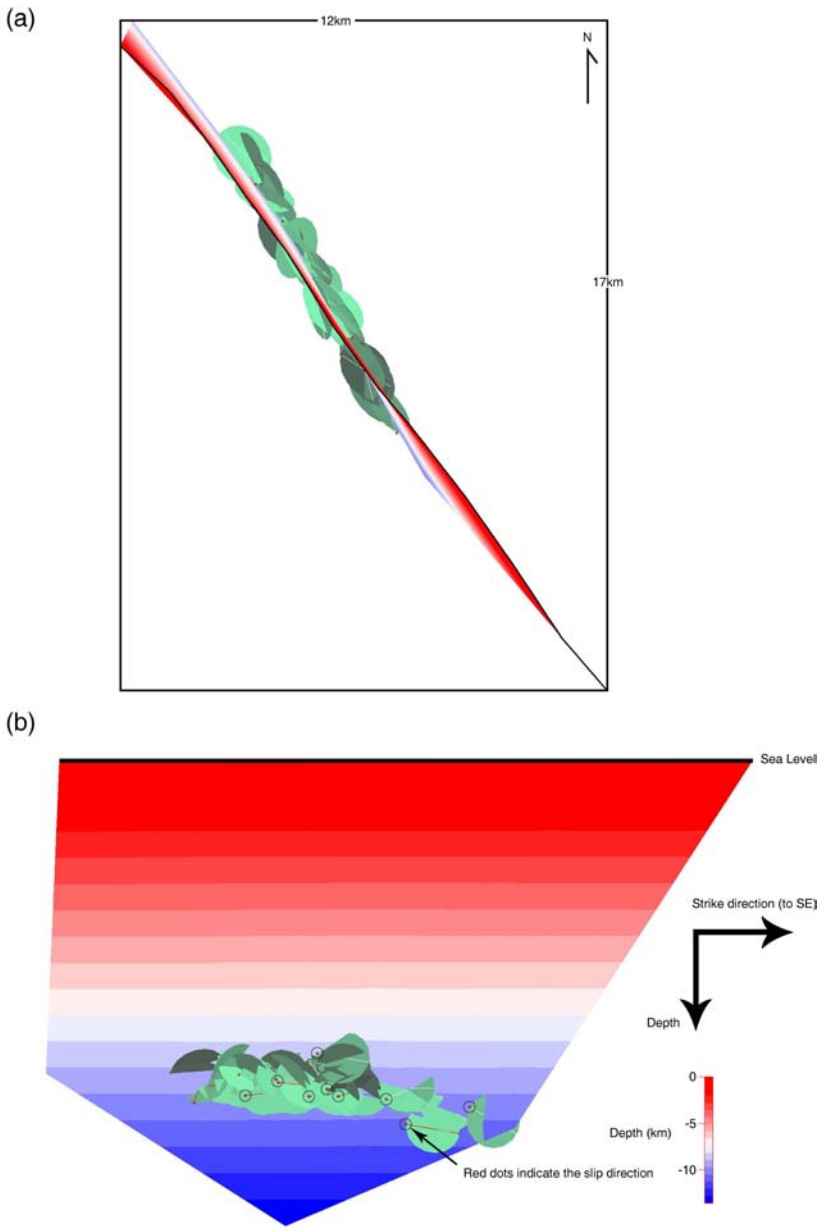

Figure 5. Map view (a) and vertical view (b) of Imperial fault surface and selected nodal planes showing the agreement between them. In (b), the slip direction shown in red dots clearly point out to NW, indicating right-lateral slip. All planes have a default diameter of 800m.

a certain depth such as Superstition Hills, Clark and Laguna Salada faults. [Actually, for the Imperial earthquake (Mw=6.4) (Deng and Sykes, 1997) happened in 1979 therefore most aftershocks are not include in Hauksson's data, which might have the same pattern to that of the Superstition Hills fault (1987), whose aftershocks are included in the Hauksson database.]

[6]. Comments on seismic hazards:
[a]. Three catastrophic earthquakes (magnitude larger than 6) happened within 40 years in this region (Imperial Earthquake: 1940 (Mw=7.0)(not include), 1979 (Mw=6.4), Elmore Ranch

Earthquake: 1987 (Mw=6.2) and Superstition Hills Earthquake: 1987 (Mw=6.6))(Deng and Sykes, 1997), which caused distinctive surface breaks (Jennings, 1994). Based on fault models, the possible rupture areas for Superstition Hills, Elmore Ranch and Imperial faults are about 350, 95, 200 km^2, respectively (Tab.1). The forecast magnitudes of earthquakes calculated from proposed fault models agree more of less with the actual historic magnitudes (Tab.1). The fault models are based on seismicity and surface break which implies the rupture areas of the faults are minimum solutions only.

Table 1. Forecast and historic magnitudes of Superstition Hills, Elmore Ranch and Imperial faults. Rupture area is calculated from the proposed fault models. The calculation of forecast magnitudes is based on empirical equations for strike-slip fault of Wells and Coppersmith (1994).

Fault	Rupture area (km^2)	Forecast magnitude	Real Magnitude
Superstition Hills F.	348.15	6.57	6.6
Elmore Ranch F.	94.63	6.00	6.2
Imperial F.	198.11	6.32	6.6

[b]. Eighteen of the faults imaged other than these three faults have minimum fault-segment surface areas ranging between 73 and 1000 km^2. These fault segments are capable of generating earthquakes in excess of magnitude 6.

Non-technical Summary

Sixty active fault segments in Southern California have been mapped in 3D in this study to depths as great as 20km by using improved earthquake locations, surface fault traces and focal mechanisms. The majority of these faults are previously known but unmapped in 3D to the base of the seismogenic zone. The detailed 3D fault models visually illustrate the complexity of the structure framework of this region especially for the San Jacinto fault zone. The empirical calculation of rupture area of imaged 3D fault segments gives us a reasonable estimate of the magnitudes of future catastrophic earthquakes as shown by the historic Superstition Hills, Elmore Ranch and Imperial earthquakes. A third of the mapped fault segments are capable of generating earthquakes in excess of magnitude 6.

Reports Published

S. Carena, J. Suppe and H. Kao, 2003, Continuity of the San Andreas fault between Cajon Pass and San Gorgonio Pass, California. Journal of Geophysical Research (in review)

Data Availability

The original earthquake hypocenter locations and focal mechanisms are available from the Southern California Earthquake Center database (http://www.scecdc.scec.org/catalogs.html). ASCII files of the clustered locations and all the Gocad files (earthquake hypocenters, focal mechanisms, and fault surfaces) are available from Li-Fan Yue (lyue@princeton.edu) and will be available through the SCEC Community Fault Model upon publication.